Supplementary Information for:

Methane-oxygen electrochemical coupling in an ionic liquid: a robust sensor for simultaneous quantification

Z. Wang,[a] M. Guo, [a] G. A. Baker, [b] J. Stetter, [c] L. Lin, [a] A. Mason[d] and X. Zeng * [a]

[a] Department of Chemistry, Oakland University, Rochester, MI 48309

[b]Department of Chemistry, University of Missouri-Columbia, Columbia, MO 65211

[c] KWJ Engineering Incorporated, 8440 Central Avenue [suite 2B or 2D], Newark, CA 94560

* To whom correspondence should be addressed. E-mail: zeng@oakland.edu

1 Experimental section

1.1 Reagents and Methods

Butyl-1-methylpyrrolidinium bis(trifluoromethylsulfonyl)imide ($[C_4mpy][NTf_2]$) (Figure S1) was prepared by standard literature procedures[1-3] and its physical properties are listed in Table S1. Polycrystalline platinum (Pt) disk, 0.5 and 1.0-mm Pt wire, and 100-mesh Pt gauze were purchased from Sigma-Aldrich (St. Louis, MO). High purity (99.99%) gases (i.e., air, nitrogen, methane, carbon dioxide, NO_2, NO, and SO_2) in which the dry air has the following composition: 78% nitrogen**,** 21% oxygen, 0.03% CO_2, 0.93% Ar and less than 0.03% of various other components) from Airgas Great Lakes (Independence, OH) were used in this study.

Table S1. Summary of Physical Properties for $[C4mpy][NTf_2]$[a]

IL	η(25 °C)/ mPs s	Λ/ S m^{-1}	d/ g cm^{-3}	V_m/ cm^3 mol^{-1}	Potential Window/ V
$[C_4mpy][NTf_2]$	76,[4] 56[5]	0.29[6]	1.41[7]	317[4]	–3.0 to +3.0[7]

[a] η is the viscosity. Λ is the conductivity. d is the mass density (±1%). V_m is the molar volume (±1%).

1.2 Electrochemical sensor set-up and characterization

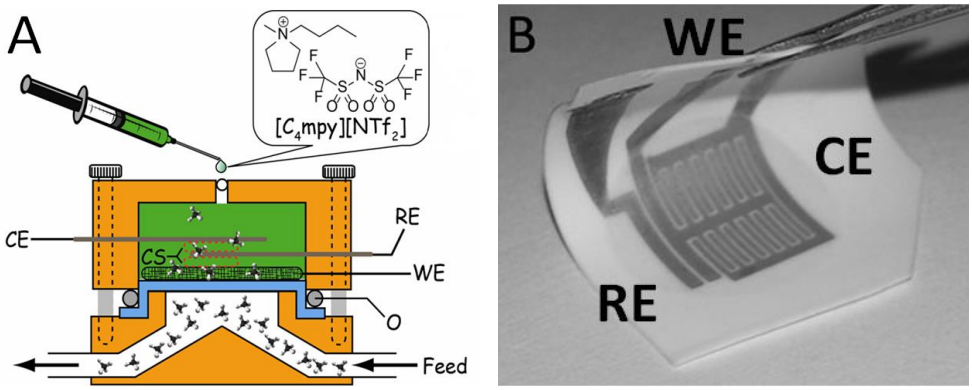

Figure S1. (A) Macroelectrode in modified Clark cell with figure abbreviations as follows: porous cellulose spacer (CS); O-ring (O); Pt reference electrode (RE); Pt working electrode (WE), Pt counter electrode (CE); inset: structure of Butyl-1-methylpyrrolidinium bis(trifluoromethylsulfonyl)imide (B) Photo of the Pt flexible interdigited electrode (IDE) on the Teflon gas-permeable membrane.

The modified Clark cell[8, 9] (Figure S1A) equipped with the platinum electrode and the microfabricated Pt electrode (Figure S1B) were used. This electrode design allows methane to be oxidized at the gas/solid/liquid interface (TPB) which minimizes the limitation of high viscosity of ILs and enable us to obtain fast response time.[10] All potentials were referenced to the platinum quasi reference electrode potential which has been calibrated with ferrocene/ferrocenium (Fc/Fc+) redox processes in the same IL for the calibration of the redox potentials throughout this study (Figure S2)[11-14]. Since 5.0 vol.% methane is the lower explosion limits in air, the tested concentration range is focused at 0-5 vol.% methane. The total gas flow was controlled at 200 sccm by digital mass-flow controllers (MKS Instruments Inc). The characterization of the

electrochemical methane sensor was performed with a VersasStatMC (Princeton AMETEK US) and detail methods can be seen in supporting information. We pre-mix various gases with a 1.25 inch stirring fan in a 125 ml glass bottle, then the mixed gases were introduced into the ionic liquid electrochemical gas sensor system. The different concentrations of mixing gases were prepared using digital mass-flow controllers that provides accurate control of the flow rate of the analyte gas flow and the diluent gas flow. All gases we used in this work are 99.95% of the purity. The accuracy of the digital mass-flow controller is ± 1% of full scale of flow rate and the repeatability is 0.2% of full scale. Either the analyte gas flow or the dilutant gas flows were humidified by bubbling it through a wash bottle filled with water. The final relative humidity (RH) of mixing gas is the ratio of humidified gas flow in the total flow rate. (Humidified gas flow/total flow rate)

Figure S1(A) illustrates the details of the amperometric gas sensor set-up used in this study. Details of this set-up are also discussed in our early report.[8] It resembles the earliest electrochemical gas sensors such as Clark cell but there are several differences. 100-mesh platinum gauze (100-mesh, Sigma-Aldrich; area of working electrode is 0.64 cm^2) was pressed onto a porous Teflon membrane (Zitex TM, Chemplast, Incorporated, Wayne, New Jersey) to serve as the working electrode, allowing for efficient current collection with excellent gas diffusivity. Two 0.5-mm diameter polycrystalline platinum wires (Sigma-Aldrich) were used as counter and quasi-reference electrodes. These electrodes were organized into a sandwich structure in the Kel-F electrochemical cell (Figure S1A) with an IL as the electrolyte and placed in a home-made dry box. All experiments were carried out at 25 ± 1 °C.

The flexible interdigited electrode (IDE) which was microfabricated planar Pt electrode on the Teflon gas-permeable membrane using method reported[15] is shown in Figure S1 (B). A

working electrode (WE) and a counter electrode (CE) are configured as interdigitated electrodes. A reference electrode is placed along the working electrode. The finger width and the gap between the CE and WE are both 200µm. The thickness of platinum was 500nm, ensured good continuity of the thin film without blocking the pores. The electrodes were coated with 200 µm $[C_4mpy][NTf_2]$.

The characterization of the electrochemical methane sensor was performed with a VersasStatMC (Princeton AMETEK US). All potentials were referenced to the platinum quasi reference electrode potential which has been calibrated with ferrocene/ferrocenium (Fc/Fc+) redox processes in the same IL for the calibration of the redox potentials throughout this study (Figure S2)[11-14]. All potentials were subsequently referenced with an error bar within ±5 mV.

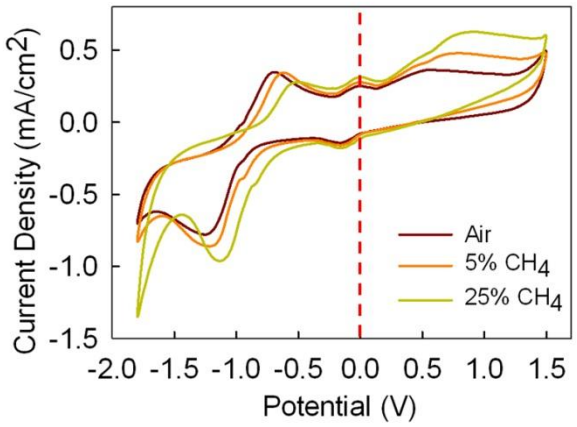

Figure S2. Potential calibration of CV in $[C_4mpy][NTf_2]$ with 1mM Fc+/Fc electrochemical redox probe. Scan rate is 500 mV s^{-1}

All the mixing gases were made by pre-mixing various gases in a glass bottle with a stirring fan before introducing them in the sensor system. Humidified gas streams were obtained by directing nitrogen gas of known flow rate through a Dreschel bottle (250 mL) partially filled with water prior to mixing with the gas analytes. Teflon tubing was used for the gas feeding system. The tail gases was absorbed by the alkali solution (NaOH and $Ca(OH)_2$).

1.3 Chronoamperometry experimental conditions

Double potential step chronoamperometry A 0.9 V of potential was applied near the methane oxidation potential for 300s and then it was stepped to -1.2V to allow oxygen reduction for 300s as well. The same potential program was repeated five times at different methane concentrations (from 1-5 vol.% in air).

Single potential step chronoamperometry A potential of 0.9 V was applied to the Pt working electrode. After a 300s current decline, at which point charging current become negligible, the sensor was exposed to an air stream with methane introduced at increasing amounts with the concentration of 1 vol.% at each step. The background current without methane is offset to zero. In these experiments, dry air was used as carrier gas and the overall gas flow rate was 200 sccm.

2 Supplementary Data

2.1 potential windows

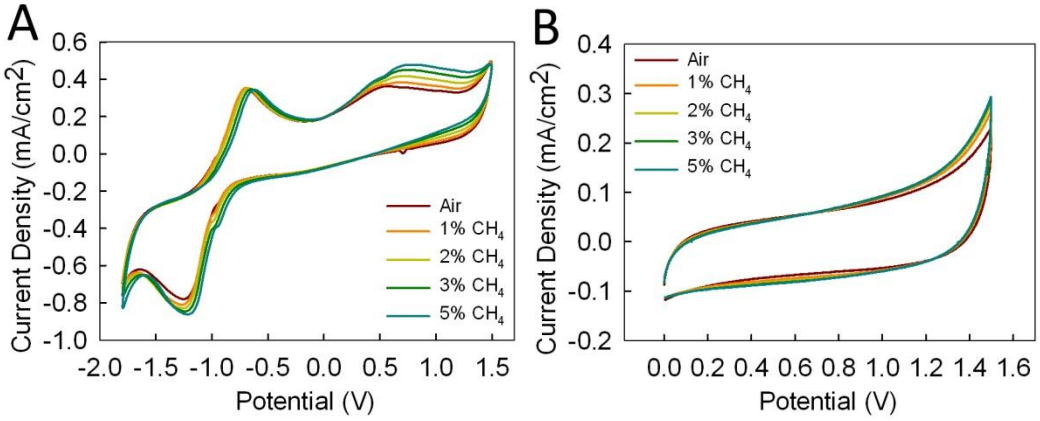

Figure S3. Peak currents density vs. potential curves at different methane concentrations in $[C_4mpy][NTf_2]$ at Pt macroelectrode, 500 mV s^{-1} scan rate (A) methane oxidation with the presence of oxygen reduction process in a wide potential window from -1.8V~1.5V; (B) methane oxidation without oxygen reduction process in a potential window from 0~1.5V.

ILs permit the facile methane electrooxidation to CO_2 and water at room temperature.[9] $[C_4mpy][NTf_2]$ is one of the best solvents to stabilize superoxide inside, which promotes the complete oxidation of methane to CO_2 and water.[16] This was supported by the results shown in Figure S3B that without superoxide, the potential of methane oxidation is higher than 1.2V and the anodic currents are much smaller. Water generated at the Pt surface also can facilitate methane oxidation to CO_2 via formation of a Pt–OH intermediate.[17, 18]

2.2 H_2O and CO_2 effect

Water has been discussed as a major potential interference for IL based system. The $[C_4mpy][NTf_2]$ used is hydrophobic which significantly minimized the amount of water adsorbed in this IL from the atmosphere. The reaction of water and superoxide radicals (O2•−) is kinetically slow in aprotic condition.[19, 20] As shown in Figure S5, the currents changes of the oxygen redox processes due to high humidity (RH: 30% or 50%), were very small compared with the dry air conditions, because of the low solubility of H_2O in this IL and high stability of O_2^- in both neutral aqueous media and this IL.

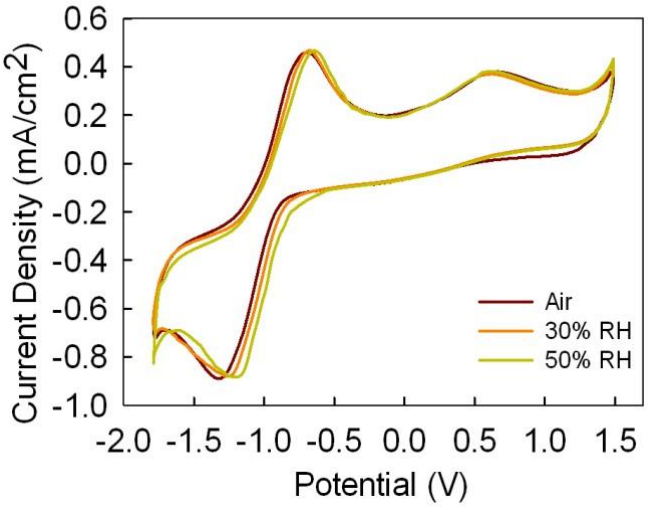

Figure S4. The effect of different H_2O concentraions towards oxygen redox process in air. (RH: relative humility in air)

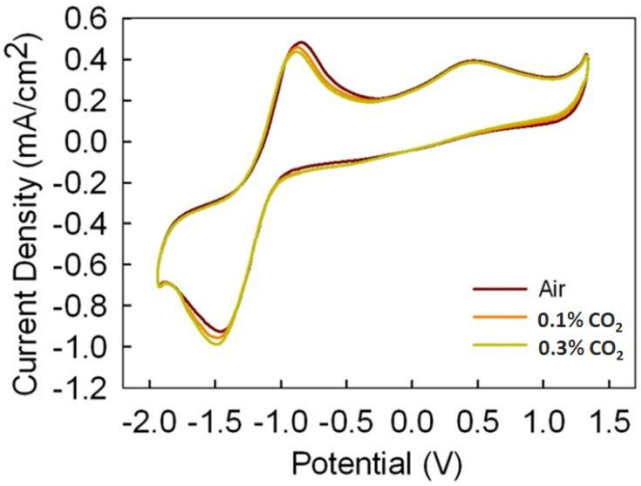

Figure S5. The effect of different CO_2 concentraions towards oxygen reduction process in air in $[C_4mpy][NTf_2]$.

2.3 Time constant determination in potential step

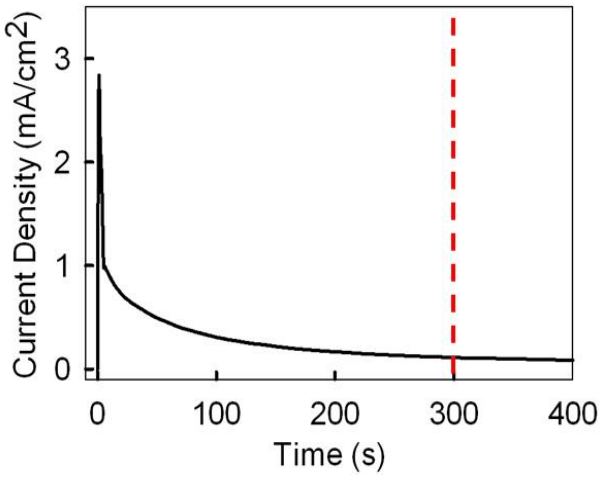

Figure S6. Potential step experiment from 0 V to 0.9 V at 100% air in [C_4mpy][NTf_2]. Time constant τ= 0.37E/Rs= 6 second, And 300 s is the 50 times of τ.

Table S2 Henry constants of gases in [C_4mpy][NTf_2]

IL	CO_2	O_2	H_2O	CH_4
[C_4mpy][NTf_2]	4.0 ± 0.3 Mpa[21]	23.6 ± 0.05 Mpa[22]	24.6 ± 0.05 Mpa[23]	N/A

References for supporting information

1. Kilaru, P., Baker, G.A. & Scovazzo, P. Density and Surface Tension Measurements of Imidazolium-, Quaternary Phosphonium-, and Ammonium-Based Room-Temperature Ionic Liquids: Data and Correlations. *J. Chem. Eng. Data* **52**, 2306-2314 (2007).
2. Burrell, A.K., Sesto, R.E.D., Baker, S.N., McCleskey, T.M. & Baker, G.A. The large scale synthesis of pure imidazolium and pyrrolidinium ionic liquids. *Green Chem.* **9**, 449-454 (2007).
3. Baker, S.N., McCleskey, T.M., Pandey, S. & Baker, G.A. Fluorescence studies of protein thermostability in ionic liquids. *Chem Commun*, 940-941 (2004).
4. Jin, H. et al. Physical properties of ionic liquids consisting of the 1-butyl-3- methylimidazolium cation with various anions and the bis(trifluoromethylsulfonyl)imide anion with various cations. *J. Phys. Chem. B* **112**, 81-92 (2008).
5. Rooney, D., Jacquemin, J. & Gardas, R., Vol. 290. (ed. B. Kirchner) 185-212 (Springer Berlin / Heidelberg, 2010).
6. Matsumoto, H. et al. The application of room temperature molten salt with low viscosity to the electrolyte for dye-sensitized solar cell. *Chem Lett*, 26-27 (2001).
7. MacFarlane, D.R., Meakin, P., Sun, J., Amini, N. & Forsyth, M. Pyrrolidinium imides: A new family of molten salts and conductive plastic crystal phases. *J. Phys. Chem. B* **103**, 4164-4170 (1999).
8. Wang, Z., Lin, P., Baker, G.A., Stetter, J. & Zeng, X. Ionic Liquids as Electrolytes for the Development of a Robust Amperometric Oxygen Sensor. *Anal Chem* **83**, 7066-7073 (2011).
9. Wang, Z. & Zeng, X. Bis(trifluoromethylsulfonyl)imide (NTf2)-Based Ionic Liquids for Facile Methane Electro-Oxidation on Pt. *J Electrochem Soc* **160**, H604-H611 (2013).
10. Jacquinot, P., Müller, B., Wehrli, B. & Hauser, P.C. Determination of methane and other small hydrocarbons with a platinum-Nafion electrode by stripping voltammetry. *Anal. Chim. Acta* **432**, 1-10 (2001).
11. Xiao, C.H., Rehman, A. & Zeng, X.Q. Dynamics of Redox Processes in Ionic Liquids and Their Interplay for Discriminative Electrochemical Sensing. *Analytical Chemistry* **84**, 1416-1424 (2012).
12. Taylor, A.W., Puttick, S. & Licence, P. Probing solvation in ionic liquids via the electrochemistry of the DPPH radical. *J Am Chem Soc* **134**, 15636-15639 (2012).

13. Lu, X.Y., Burrell, G., Separovic, F. & Zhao, C. Electrochemistry of Room Temperature Protic Ionic Liquids: A Critical Assessment for Use as Electrolytes in Electrochemical Applications. *J Phys Chem B* **116**, 9160-9170 (2012).
14. Pool, D.H. et al. Acidic ionic liquid/water solution as both medium and proton source for electrocatalytic H-2 evolution by [Ni(P2N2)(2)](2+) complexes. *P Natl Acad Sci USA* **109**, 15634-15639 (2012).
15. Wang, Z. et al. Methane Recognition and Quantification by Differential Capacitance at the Hydrophobic Ionic Liquid-Electrified Metal Electrode Interface. *Journal of The Electrochemical Society* **160**, B83-B89 (2013).
16. Bond, G.C. & Thompson, D.T. Gold-catalysed oxidation of carbon monoxide. *Gold Bull* **33**, 41-51 (2000).
17. Watanabe, M. & Uchida, H. in Fuel Cell Catalysis 317-341 (John Wiley & Sons, Inc., 2008).
18. Koper, M.T.M., Lai, S.C.S. & Herrero, E. in Fuel Cell Catalysis 159-207 (John Wiley & Sons, Inc., 2008).
19. Damjanovic, A., Genshaw, M.A. & Bockris, J.O.M. The mechanism of oxygen reduction at platinum in alkaline solutions with special referens to HO2 2. *J. Electrochem. Soc.* **114**, 1107-1112 (1967).
20. Pletcher, D. & Sotiropoulos, S. Hydrogen adsorption-desorption and oxide formation-reduction on polycrystalline platinum in unbuffered aqueous solutions. *Journal of the Chemical Society, Faraday Transactions* **90**, 3663-3668 (1994).
21. Tagiuri, A., Sumon, K.Z., Henni, A., Zanganeh, K. & Shafeen, A. Effect of cation on the solubility of carbon dioxide in three bis(fluorosulfonyl)imide low viscosity ([FSI]) ionic liquids. *Fluid Phase Equilibr* **375**, 324-331 (2014).
22. Katayama, Y., Sekiguchi, K., Yamagata, M. & Miura, T. Electrochemical Behavior of Oxygen/Superoxide Ion Couple in 1-Butyl-1-methylpyrrolidinium Bis(trifluoromethylsulfonyl)imide Room-Temperature Molten Salt. *J Electrochem Soc* **152**, E247-E250 (2005).
23. Freire, M.G. et al. Mutual Solubilities of Water and Hydrophobic Ionic Liquids. *The Journal of Physical Chemistry B* **111**, 13082-13089 (2007).